Organic & Biomolecular Chemistry

Cite this: *Org. Biomol. Chem.*, 2011, **9**, 1133

www.rsc.org/obc

PAPER

New hedgehog/GLI-signaling inhibitors from *Adenium obesum*†

Midori A. Arai,*[a] Chikashi Tateno,[a] Takashi Koyano,[b] Thaworn Kowithayakorn,[c] Seiichiro Kawabe[d] and Masami Ishibashi*[a]

Received 6th September 2010, Accepted 1st November 2010
DOI: 10.1039/c0ob00677g

The aberrant hedgehog (Hh)/GLI signaling pathway causes the formation and progression of a variety of tumors. We recently constructed a cell-based screening system to search for Hh/GLI signaling inhibitors from natural resources. Using our screening system, *Adenium obesum* was found to include Hh/GLI signaling inhibitors from our tropical plant extract libraries. Bioassay-guided fractionation of this plant extract led to the isolation of 17 cardiac glycosides (**1**–**17**), including 3 new compounds (**4**, **9**, **16**). These compounds showed strong inhibitory activities, especially the IC_{50} of **17** is 0.11 μM. The inhibition of GLI-related protein expression with **3**, **9**, **11**, **15** and **17** was observed in human pancreatic cancer cells (PANC1), which express Hh/GLI components aberrantly. The expressions of GLI-related proteins PTCH and BCL2 were clearly inhibited. These compounds also showed selective cytotoxicity against two cancer cell lines, with less effect against normal cells (C3H10T1/2). RT-PCT examinations showed that *Ptch* mRNA expression by **3**, **11**, **15** and **17** was inhibited.

Introduction

The hedgehog (Hh)/GLI signaling pathway has recently been implicated in several tumors,[1,2] such as skin,[3] brain,[4] prostate,[5] digestive tract,[6] pancreas,[7] and lung.[8] The vertebrate Hh family includes three members: sonic Hh (Shh), desert Hh, and indiana Hh, which all bind to the same receptor, Patched (PTCH). In the absence of Hh ligand, PTCH interacts with Smoothend (Smo) to inhibit its function, preventing activation of the downstream signaling cascade. Upon Hh binding, Smo inhibition is released, resulting in activation of the downstream signaling cascade through the release of the transcriptional factor GLI from a macromolecular complex on microtubules (Fig. 1). In some types of human tumors, Hh/GLI signaling is constitutively activated because of mutations in PTCH or SMO, leading to tumor formation and progression. Thus, targeted Hh/GLI signaling is anticipated as an effective cancer therapeutic strategy.[9] Cyclopamine has been identified as an inhibitor of Hh signaling by binding to SMO,[10,11] and other types of SMO antagonists have been reported, such as Cur-61414[12] and SANTs.[13] In addition, several small-molecule inhibitors of Hh signaling inhibitors, including GLI-mediated transcription inhibitors (GANTs),[14] inhibitor of class IV alcohol dehydrogenase (JK184)[15] and a small molecule that binds Shh protein (robotnikinin),[16] have been reported, but there is still an urgent need to identify different types of GLI-mediated transcriptional inhibitors.

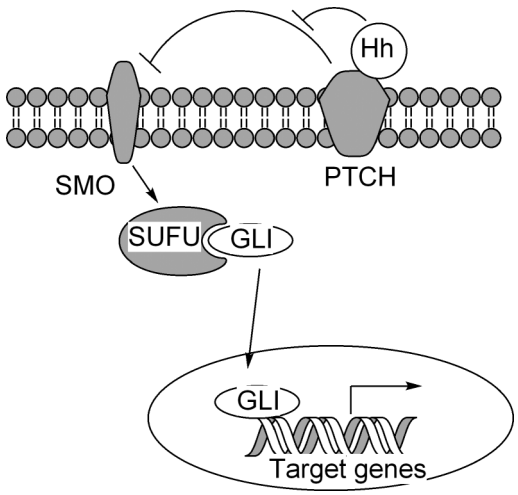

Fig. 1 Hedgehog/GLI-mediated signaling pathway.

To discover inhibitors of the Hh/GLI signaling pathway from natural resources, we have recently reported the construction of a cell-based screening assay system for the Hh/GLI signaling pathway (Fig. 2).[17] This is an assay using a GLI-dependent luciferase reporter in human keratinocyte cells (HaCaT) expressing GLI1 under tetracycline control (T-REx system). The 12 consecutive GLI-binding sites (12×GACCACCCA) and the TK promoter were inserted into the pGL4.20 plasmid (Promega). The constructed plasmid, pGL4-GLI BS, was stably transfected into HaCaT cells expressing exogenous GLI1 protein under

[a]*Graduate School of Pharmaceutical Sciences, Chiba University, 1-33 Yayoi-cho, Inage-ku, Chiba 263-8522, Japan. E-mail: marai@p.chiba-u.ac.jp; Fax: +81 43 290 2913*
[b]*Temko Corporation, 4-27-4 Honcho, Nakano, Tokyo 164-0012, Japan*
[c]*Faculty of Agriculture, Khon Kaen University, Khon Kaen 40002, Thailand*
[d]*College of Life Science, 2640 Nishinoura, Tsurajima-cho, Kurashiki University of Science and the Arts, Kurashiki, Okayama 712-8505, Japan*
† Electronic supplementary information (ESI) available. See DOI: 10.1039/c0ob00677g

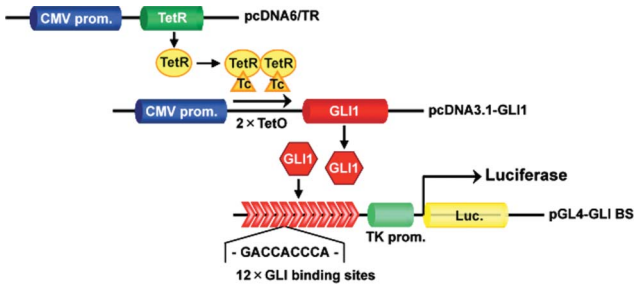

Fig. 2 The assay system with T-REx (tetracycline-regulated expression system). pcDAN3.1-GLI1 expresses exogenous GLI1 protein by tetracycline-regulated CMV promoter, and GLI1 binds to GLI binding site on pGL4-GLI BS. Tetracycline removes TetR to start GLI1 expression. Tc, tetracycline; TetR, tetracycline repressor; TetO, tetracycline operator; CMV, cytomegalovirus promoter; GLI1, transcriptional factor of Hh/GLI signaling pathway.

tetracycline control. During the screening of natural resource libraries, including plant extracts and actinomycete extracts with the assay system, we identified some natural products and natural plant extracts as GLI1-mediated transcriptional inhibitor samples. Among them, we chose the methanol extract of *Adenium obesum* to examine active components, and isolated 17 GLI-mediated transcriptional inhibitors, including 3 new compounds. Finally, we determined the effect of these inhibitors on protein expression related to the Hh/GLI signaling pathway.

Results and discussion

The methanol extract of *A. obesum* was partitioned successively with EtOAc, *n*BuOH, and water. The active EtOAc layer was subjected to silica gel column chromatography and Sephadex LH-20 column chromatography and further purification by reversed-phase HPLC to yield 12 active compounds (**1**–**12**), including 2 new compounds (**4**, **9**). The 10 isolated compounds were identified as digitoxigenin (3β,14-dihydroxy-5β-card-20(22)-enolide) (**1**),[18] 16-acetylgitoxigenin 2′-*O*-acetyl-β-D-thevetoside (3β,5β,16β-3-[(2-*O*-acetyl-β-D-thevetosyl)oxy]-16-acetyloxy-14-hydroxy-card-20(22)-enolide) (**2**),[19] gitoxigenin β-D-sarmentoside (**3**),[20] 16-acetylgitoxigenin β-D-sarmentoside (**5**),[20] digitoxigenin 2′-*O*-acetyl-β-D-thevetoside (**6**),[19] digitoxigenin β-D-sarmentoside (**7**),[21] gitoxigenin β-D-thevetoside (**8**),[19] 16-acetylgitoxigenin β-D-thevetoside (**10**),[22] digitoxigenin β-D-digitaloside (**11**),[23] and digitoxigenin β-D-thevetoside (**12**)[24] on the basis of comparisons with their spectral data in the literature (Fig. 3). The active *n*BuOH layer was also subjected to silica gel column chromatography, followed by ODS-HPLC to yield 5 active compounds (**13**–**17**), including 1 new compound (**16**). The 4 isolated compounds were identified as gitoxigenin β-D-glucosyl-(1→4)-β-D-thevetoside (**13**),[22] 16-anhydrogitoxigenin β-D-glucosyl-(1→4)-β-D-thevetoside (**14**),[22] 16-acetylgitoxigenin β-D-glucosyl-(1→4)-β-D-thevetoside (**15**),[22] and digitoxigenin β-D-glucosyl-(1→4)-β-D-thevetoside (**17**) [22]

Compound **4** was obtained as a white powder. The HRFAB-MS spectrum suggested a molecular formula of $C_{31}H_{46}O_9$. The ^{13}C NMR spectrum displayed 31 carbon resonances (Table 1). A carbonyl carbon resonance at δ 174.1, and two olefin carbon resonances were located at δ 169.6 and 121.9. An ester carbon was detected at δ 161.2. Three resonances for carbons bearing oxygen were observed at δ 73.3, 74.6, and 83.4 in addition to one methoxy methyl and four oxygenated carbon resonances of a 2,6-dideoxyhexose sugar. In the ^1H NMR spectra, a signal due to the anomeric proton of β-linked hexose, protons of one methoxy and one *sec*-methyl group of the sugar portion were observed. The comparison of the ^1H and ^{13}C NMR spectrum as gitoxigenin β-D-sarmentoside (**3**) suggested that compound **4** has gitoxigenin as aglycon and β-D-sarmentoside as the sugar portion. The HMBC correlation between δ 8.19 and 74.6 ppm (C-16) indicated a formic ester at C-16 (Fig. 4). The HMBC correlations [carbonyl carbon at δ 174.1 with olefinic H-22 (δ 6.32); olefinic methine carbon C-22 (δ 121.9) with H-17 and H-21; quaternary olefinic C-20 (δ 169.6) with H-16, H-17 and H-21] showed the structure of the γ-lactone moiety and the connection of its C-20 position at C-17. The connected position of sugar was also indicated by the HMBC correlation between anomeric proton and 73.3 ppm (C-3). The structure of **4** is 16-formylgitoxigenin β-D-sarmentoside.

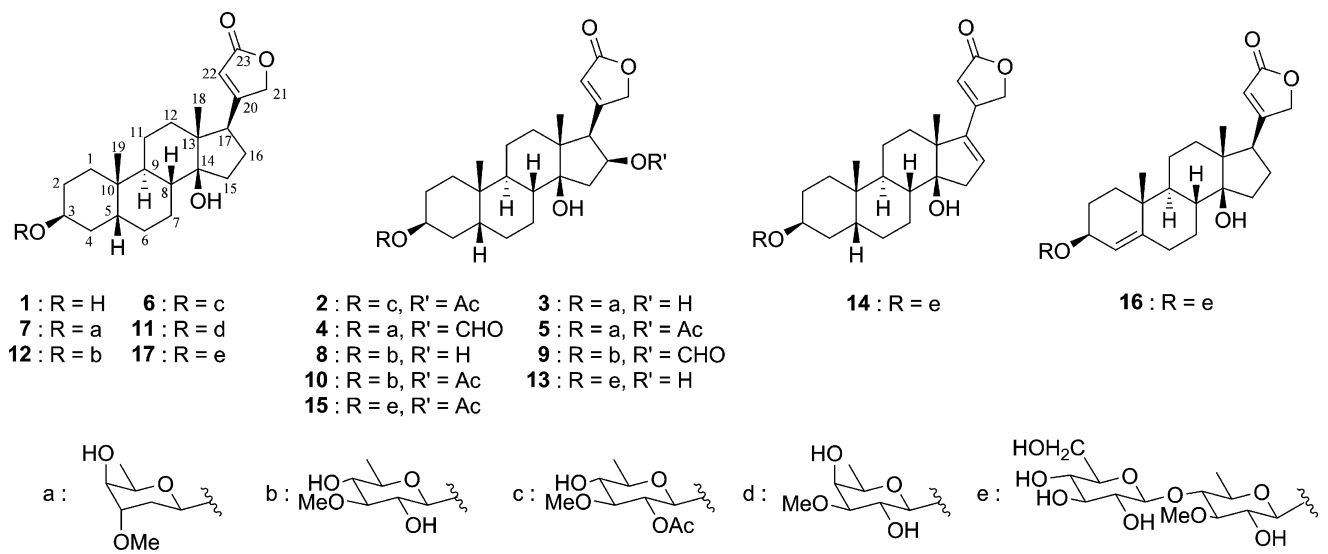

Fig. 3 Hedgehog/GLI-mediated inhibitors from *Adenium obesum*.

Table 1 ^{1}H and ^{13}C NMR data of compounds **4**, **9** and **16** (δ in ppm, J in Hz; in pyridine-d_5)

	4[a]		**9**[a]		**16**[b]	
no.	δ_H (J in Hz)	δ_C	δ_H (J in Hz)	δ_C	δ_H (J in Hz)	δ_C
1		30.7		30.5[c]	1.26 m	35.9
					1.64 m	
2		27.2[c]		27.0	2.13 m	27.9
3	4.31 br s	73.3	4.34 br s	74.6	4.47 m	75.0
4		30.8		30.7[c]	5.62 s	122.1
5		37.1	2.03 m	36.6		146.3
6		27.1[c]		27.0	1.98 m	32.6
7	2.11 m	21.1		21.1	1.12 m	29.1
					2.33 m	
8		41.9		41.9	1.74 m	42.1
9		35.8		35.8	1.04 m	50.3[c]
10		35.5		35.4		37.7
11		21.7		21.6	1.23 m	21.3
					1.35 m	
12		38.8		38.8	1.38 m	39.5
					1.23 m	
13		50.6		50.5		49.9[c]
14		83.4		83.4		84.3
15	2.04 dd (15.2, 2.1)	41.5	2.08 m	41.5	1.79 m	33.1
	2.83 dd (15.6, 10.0)		2.82 dd (15.4, 10.0)			
16	5.79 m	74.6	5.78 ddd (10.0, 8.8, 1.7)	74.6	2.06 m	27.2
17	3.40 d (8.5)	56.8[d]	3.40 d (8.8)	56.7	2.76 dd (8.9, 5.2)	51.2
18	1.06 s	16.3	1.05 s	16.2	1.02 s	16.1
19	0.89 s	23.9	0.79 s	23.7	0.88 s	18.9[d]
20		169.6		169.6		175.9
21	5.28 dd (18.3, 1.6)	76.2	5.27 dd (18.3, 1.7)	76.2	5.02 dd (18.1, 1.5)	73.7
	5.46 dd (18.3, 1.6)		5.45 dd (18.3, 1.7)		5.30 dd (18.1, 1.5)	
22	6.32 s	121.9	6.32 br s	121.9	6.12 br s	117.7
23		174.1		174.1		174.5
16-OCHO	8.19 s	161.2	8.19 s	161.2		
1′	5.14 dd (10.0, 1.5)	97.5	4.80 d (7.8)	103.0	4.85 d (7.9)	103.0
2′	2.11 m	32.2	3.99 m	75.1		74.8
	2.37 ddd (13.3, 10.0, 2.9)					
3′	3.83 m	80.2	3.63 t (8.5)	88.2	3.78 t (9.0)	86.3
4′	3.74 br d (4.6)	67.8	3.67 m	76.0	3.74 br d (4.6)	83.4
5′	4.16 q (6.6)	70.0	3.73 m	72.7	3.82 m	72.0[e]
6′	1.50 d (6.6)	17.5	1.60 d (6.1)	18.7	1.80 d (6.1)	18.8[d]
3′-OMe	3.34 s	56.7[d]	3.89 s	60.9	3.97 s	60.6
1″					5.17 d (7.9)	104.9
2″					4.05 m	75.9
3″						78.7
4″						71.9[e]
5″						78.1
6″					4.37 dd (11.9, 4.2)	63.1
					4.53 br d (11.9)	

[a] 400 MHz for ^{1}H and 100 MHz for ^{13}C. [b] 500 MHz for ^{1}H and 125 MHz for ^{13}C. [c] These signals may be reversed. [d] These signals may be reversed. [e] These signals may be reversed.

Compound **9** was obtained as a white powder. The HRFAB-MS spectrum suggested a molecular formula of $C_{31}H_{46}O_{10}$. The ^{13}C NMR spectrum displayed 31 carbon resonances (Table 1). The comparison of the ^{1}H and ^{13}C NMR spectrum as gitoxigenin β-D-thevetoside (**8**) suggested that compound **9** has gitoxigenin as aglycon and β-D-thevetoside as the sugar portion. The HMBC correlations supported the structures (Fig. 4); the γ-lactone moiety, a formic ester at C16, and the sugar moiety and its connected position. Hydrolysis of **9** afforded D-thevetose, which was identified by comparison of $[\alpha]_D^{19}$ data (+22.9, *c* 0.50, H_2O) with the literature (+36, H_2O).[25] The structure of **9** is 16-formylgitoxigenin β-D-thevetoside.

Compound **16** was obtained as a white powder. The HRFAB-MS spectrum suggested a molecular formula of $C_{36}H_{54}O_{13}$. The ^{13}C NMR spectrum displayed 36 carbon resonances (Table 1). The comparison of the ^{1}H and ^{13}C NMR spectrum as digitoxigenin β-D-glucosyl-(1→4)-β-D-thevetoside (**17**) suggested that compound **16** has the same sugar portion. The HMBC correlations (Fig. 4) [carbon at C-2 (δ 27.9), C-6 (δ 32.6), and C-10 (δ 37.7) with olefinic H-4 (δ 5.62); quaternary olefinic C-5 (δ 146.3) with H-19] indicated the canariengenin (3β,14-dihydroxy-carda-4,20(22)-dienolide) aglycon. The HMBC correlations and the COSY spectra supported the aglycon structures. Thus, the full structure of **16** is canariengenin β-D-glucosyl-(1→4)-β-D-thevetoside.

Compounds **3**, **9**, **11**, **15**, and **17** dose-dependently inhibited GLI1-mediated transcriptional activity with little effect on cell viability (Fig. 5), while **9** showed cytotoxity at 0.25 μM. The IC_{50} values of **3**, **9**, **11**, **15**, and **17** against GLI1-mediated

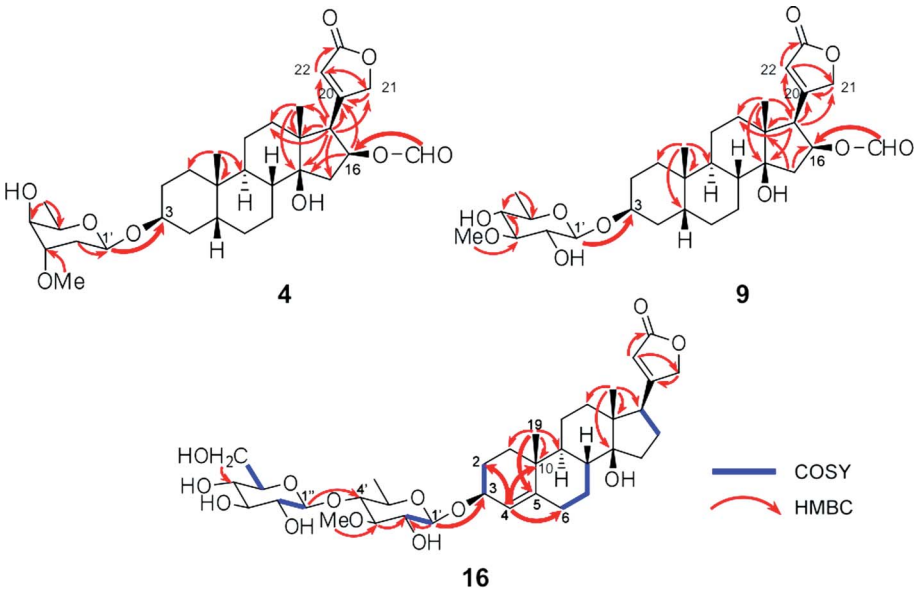

Fig. 4 Key HMBC and ^{1}H–^{1}H COSY data for compounds (**4**, **9**, **16**).

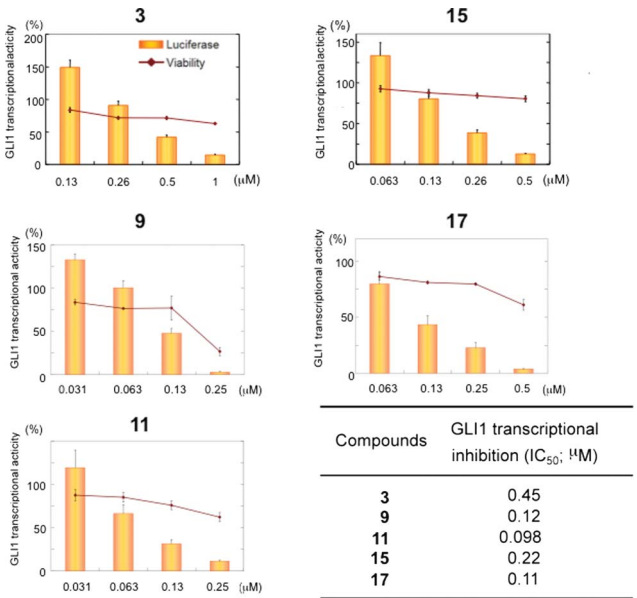

Compounds	GLI1 transcriptional inhibition (IC_{50}; μM)
3	0.45
9	0.12
11	0.098
15	0.22
17	0.11

Fig. 5 Inhibition of GLI1-mediated transcriptional activity (solid columns; reporter activity) and cell viability (solid curves) of compounds **3**, **9**, **11**, **15**, and **17**. The assays were performed at 0.05% DMSO ($n = 3$). Error bars represent SD.

transcriptional inhibitory activity were 0.45, 0.12, 0.098, 0.22, 0.11 μM, respectively. Interestingly, **3**, **9**, **11**, and **15** activated the transcription at low concentration. If they also had the character of CMV promoter activators, GLI1 expression would be accelerated in pcDNA3.1-GLI1 and then luciferase expression would increase (Fig. 2). We checked the GLI1 protein expression by Western blotting at a low concentration of **3**; however, there was no change at the GLI1 protein level (data not shown). At this stage, the reason for activation at a low concentration is unknown.

Other compounds also showed good inhibitory activity (see supplementary file). The Structure–Activity Relationship (SAR) of isolated Hh inhibitors indicated that the 16β-hydroxy, acetyloxy, and formyloxy unit decreased the activity (IC_{50}; **2** (2.4 μM), **6** (1.2 μM): **3** (0.45 μM), **7** (0.21 μM): **8** (0.50 μM), **12** (0.14 μM): **13** (2.3 μM), **17** (0.11 μM)). However, compound **9** (IC_{50} 0.12 μM) showed comparable inhibition with **12**. A modification of aglycone with a double bond also decreased the activity (IC_{50}; **14** (1.9 μM), **16** (1.8 μM)). Interestingly, there is no significant structural similarity in the reported Hh inhibitors. Our reported cardiac glycosides are the first type of Hh inhibitors.

PANC1 and DU145 express numerous Hh/GLI signaling pathway components, including PTCH, Suppressor of Fused, GLI1, and GLI2, resulting from aberrant Hh/GLI signaling in the cells. Next, we confirmed the cytotoxicity of isolated compounds against human pancreatic (PANC1) and prostate (DU145) cancer cell lines using a Fluorometric Microculture Cytotoxicity Assay (FMCA)[26] (Fig. 6). Compounds **3**, **9**, **11**, **15**, and **17** were cytotoxic against PANC1 cells with IC_{50} values of 0.50, 0.027, 0.091, 0.11, 0.17 μM, respectively. They also showed cytotoxicity against DU145 cells with IC_{50} values of 0.34, 0.041, 0.065, 0.14, 0.086 μM, respectively. A mesenchymal progenitor (C3H10T1/2) cell line derived from the mouse embryonic mesodermal was also examined, because this normal cell line is Hh responsive but not reliant on Hh for survival. No compounds showed cytotoxicity against C3H10T1/2. From the clinical point of view, these results are important because anticancer agents not affecting normal cells are favorable.

We further examined the effects on the protein expression related to Hh/GLI-mediated transcription (Fig.7). The anti-apoptosis protein Bcl2 is the target of the Hh/GLI signaling pathway. Previous studies have showed that transactivation of *bcl-2* is regulated by Hh/GLI signaling through GLI1[27] and GLI2.[28] These reports suggest that aberrant Hh/GLI signaling is related to the anti-apoptotic character of cancer cells due to enhanced expression of Bcl2 protein. A tumor suppressor PTCH expression is also known to be regulated by the Hh/GLI signaling pathway. We investigated their levels in PANC1 cells. Compound **3** showed a dose-dependent reduction of the levels of PTCH and BCL2 proteins (Fig. 7A). Compounds **9**, **11**, **15**, and **17** also clearly

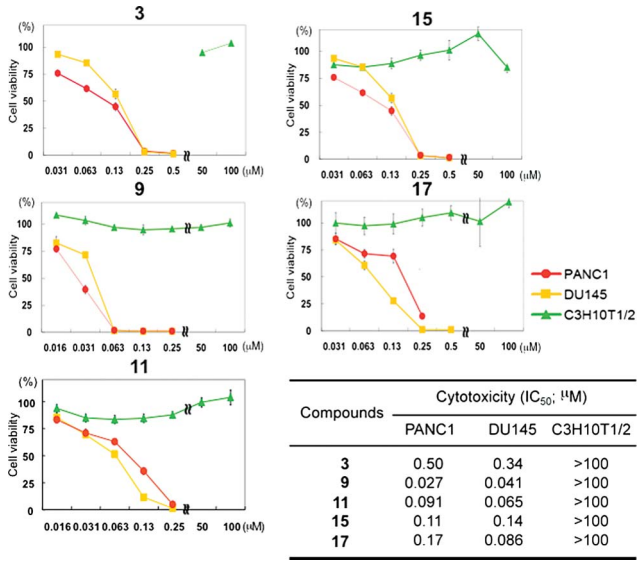

Compounds	Cytotoxicity (IC_{50}; μM)		
	PANC1	DU145	C3H10T1/2
3	0.50	0.34	>100
9	0.027	0.041	>100
11	0.091	0.065	>100
15	0.11	0.14	>100
17	0.17	0.086	>100

Fig. 6 Cytotoxic effects on PANC1, DU145, and C3H10T1/2 cells. The assays were performed at 0.05% DMSO ($n = 3$). Error bars represent SD.

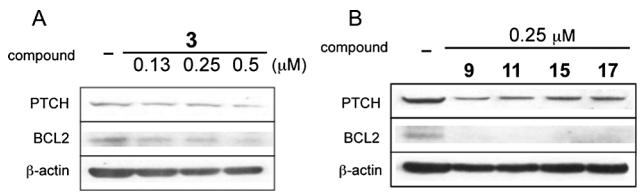

Fig. 7 Inhibition of GLI-related proteins PTCH and BCL2 in PANC1 cells. A) PTCH and BCL2 protein expression were inhibited by **3** in a dose-dependent manner. B) PTCH and BCL2 protein levels in PANC1 cells with treatment with **9**, **11**, **15**, and **17** at 0.25 μM.

decreased PTCH and BCL2 proteins at 0.25 μM in PANC1 (Fig. 7B).

Moreover, we examined the inhibition of GLI-mediated mRNA expression. Compound **3** inhibited the mRNA production of *Ptch* in PANC1 in a dose-dependent manner (Fig. 8A). Compounds **11**, **15**, and **17** also clearly decreased *Ptch* mRNA at 0.25 μM in PANC1 (Fig. 8B). These results clearly show that these compounds inhibit GLI-mediated transcription.

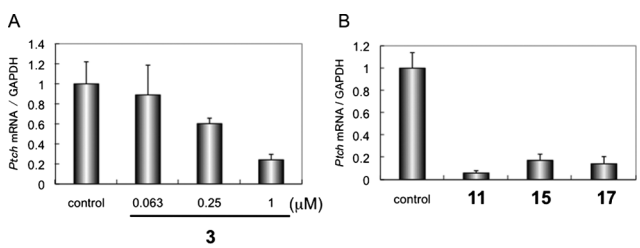

Fig. 8 Inhibition of GLI-mediated mRNA expression in PANC1 cells. A) *PTCH* mRNA expression was inhibited by **3** in a dose-dependent manner. B) *PTCH* mRNA expression with treatment with **11**, **15**, and **17** at 0.25 μM. *GAPDH* was used as an internal control. Compounds were assayed in triplicate. Error bars represent SD.

Conclusion

In conclusion, we identified 17 GLI-mediated transcriptional inhibitors, including 3 new compounds (**4**, **9**, **16**). These compounds showed cytotoxicity against cancer cells (PANC1, DU145), in which Hh/GLI signaling is aberrantly activated. The inhibitors suppressed the GLI-mediated expression of tumor suppressor PTCH and anti-apoptosis protein BCL2, and inhibited *Ptch* mRNA expression in PANC1. These compounds might be good tools and/or leads to new agents in the investigation of Hh/GLI signaling pathway inhibitors.

Experimental

General experimental procedures

FAB-MS was measured on a JEOL JMS-AX500 spectrometer, and high-resolution FABMS spectra were obtained on a JEOL JMS-HX110 spectrometer. NMR spectra were recorded on JEOL JNM GSX-A400, and A500 spectrometers with a deuterated solvent whose chemical shift was taken as an internal standard. IR spectra were measured on ATR using a JASCO FT-IR 230 spectrophotometer. UV spectra were measured using a Shimadzu UV mini-1240 spectrometer. Optical rotations were measured with a JASCO P-1020 polarimeter, and CD spectra were obtained on a JASCO J-720WI spectropolarimeter.

Plant material

The plant *Adenium obsesum* (Apocynaceae) was collected in Khon Kaen, Thailand in 1999. A voucher specimen (6-210) was deposited in our laboratory.

Extraction and isolation

The leaves (35.0 g) of *A. obsesum* were extracted with MeOH. Part (7.6 g/8.1 g) of the MeOH extract was partitioned with H_2O (200 mL) between hexane (200 mL × 3), and the aqueous phase was further extracted with EtOAc (200 mL × 3), and n-BuOH (200 mL × 1) to afford hexane extract (1.0 g), EtOAc extract (1.6 g), n-BuOH extract (0.57 g) and H_2O extract (3.6 g). In the GLI1-mediated transcriptional assay, the EtOAc extracts (0.5 μg mL^{-1}) and n-BuOH extract (1.0 μg mL^{-1}) were active, and their luciferase activities were 5% and 38%, respectively. The EtOAc extract (1.6 g) was subjected to silica gel column chromatography (20 × 510 mm), eluted with gradient mixtures of hexane–EtOAc (9/1–0/1) and EtOAc–MeOH (4/1–0/1) to give 10 fractions (frs 1A–1J). In the assay of frs 1H and 1I showed activity with high cell viability (>75%). Fr. 1H (107 mg) was separated by Sephadex LH-20 column chromatography (16 × 700 mm) eluted with $CHCl_3$–MeOH (1/1) to give 3 fractions (2A–2C). Fr. 2B (85 mg) was purified with reversed-phase HPLC (Develosil ODS-HG-5, 20 × 250 mm; eluent, H_2O–MeOH (2/3); flow rate, 5.0 mL min^{-1}) to afford **2** (1.3 mg, t_R 47 min), **3** (2.5 mg, t_R 52 min), **4** (0.9 mg, t_R 60 min), **5** (7.4 mg, t_R 71 min), **6** (9.2 mg, t_R 73 min), and active fractions 3B and 3J. Fr. 3B (3.1 mg) was subjected to reversed-phase HPLC (Inertsil ODS-3, 10 × 250 mm; eluent, H_2O–MeOH (2/3); flow rate, 1.0 mL min^{-1}) to give 4 fractions (frs 8A–8D). Fr. 8C (2.0 mg) was separated by reversed-phase HPLC (CAPCELPAK C18 ACR, 4.6 × 250 mm; eluent, H_2O–MeCN

(7/3); flow rate, 0.6 mL min^{-1}, UV 220 nm) to afford **1** (0.9 mg, t_R 43 min). Part (21 mg/24 mg) of Fr. 3 J was subjected to reversed-phase HPLC (Develosil ODS-HG-5, 20 × 250 mm; eluent, H_2O–MeOH (1/3); flow rate, 5.0 mL min^{-1}, UV 254 nm) to afford **7** (6.8 mg, t_R 25 min). Fr. 1I (711 mg) was separated by Diaion HP-20 (20 × 580 mm; eluent, MeOH/acetone (1/0–0/1) to give 3 fractions (5A–5C). Part (177 mg/549 mg) of Fr. 5A was subjected to reversed-phase HPLC (Develosil ODS-HG-5, 20 × 250 mm; eluent, H_2O–MeOH (9/11); flow rate, 5.0 mL min^{-1}) to afford **8** (1.3 mg, t_R 35 min), **9** (4.0 mg, t_R 50 min), **10** (20 mg, t_R 61 min), **11** (2.2 mg, t_R 86 min), **12** (88 mg, t_R 98 min). n-BuOH extract (0.57 g) was subjected to silica gel column chromatography (20 × 180 mm) and eluted with gradient mixtures of hexane–EtOAc (1/1–0/1) and EtOAc–MeOH (9/1–0/1) to give 6 fractions (frs 10A–10F). Fr. 10D (313 mg) was subjected to silica gel column chromatography (14 × 340 mm) and eluted with gradient mixtures of $CHCl_3$–MeOH (9/1–0/1) to give 5 fractions (frs 11A–11E). Part (74 mg/81 mg) of Fr. 11B was subjected to reversed-phase HPLC (Inertsil ODS-3, 10 × 250 mm; eluent, H_2O–MeOH (11/14); flow rate, 2.0 mL min^{-1}) to afford **13** (1.4 mg, t_R 24 min), **14** (1.1 mg, t_R 27 min), **15** (8.2 mg, t_R 32 min), **16** (0.9 mg, t_R 48 min), **17** (30 mg, t_R 50 min).

16-Formylgitoxigenin β-D-sarmentoside (4)

White amorphous solid; $[\alpha]_D^{26}$ −19.3 (*c* 0.50, MeOH); IR (ATR) ν_{max} 3503, 2935, 1732, 1170, 1094, 1029 cm^{-1}; ^{1}H and ^{13}C NMR data, see Table 1; FABMS *m/z* 585 [M + Na]$^+$; HRFABMS *m/z* 601.2745 [M + K]$^+$ (calcd for $C_{31}H_{46}O_9K$ 601.2779).

16-Formylgitoxigenin β-D-thevetoside (9)

White amorphous solid; $[\alpha]_D^{20}$ −9.9 (*c* 0.50, MeOH); IR (ATR) ν_{max} 3455, 2935, 1736, 1169, 1067, 1023, 752 cm^{-1}; ^{1}H and ^{13}C NMR data, see Table 1; FABMS *m/z* 579 [M + H]$^+$; HRFABMS *m/z* 579.3190 [M + H]$^+$ (calcd for $C_{31}H_{47}O_{10}$ 579.3169). After reflux of **9** (3.0 mg, 5.2 mmol) with dioxane (5 mL) and 5% H_2SO_4 (5 mL) for 2 h, the mixture was diluted with H_2O, and partitioned with $CHCl_3$. The H_2O layer was then deacidified with Amberlite IRA96SB and the H_2O layer was concentrated *in vacuo*. The residue (D-thevetose, 0.9 mg, 98%) showed one spot. $[\alpha]_D^{19}$ +22.9 (*c* 0.50, H_2O, 24 h) (lit. +36).[25]

Canariengenin β-D-glucosyl-(1→4)-β-D-thevetoside (16)

White amorphous solid; $[\alpha]_D^{20}$ −87.5 (*c* 0.10, pyridine); IR (ATR) ν_{max} 3447, 2936, 1734, 1715, 1061, 1029 cm^{-1}; ^{1}H and ^{13}C NMR data, see Table 1; FABMS *m/z* 733 [M + K]$^+$; HRFABMS *m/z* 733.3149 [M + K]$^+$ (calcd for $C_{36}H_{54}O_{13}K$ 733.3201).

GLI1-mediated transcriptional activity assay

In the cell-based assay system, three plasmids (pcDNA6/TR, pcDNA3.1-GLI1, and pGL4-GLI-luc) are stably co-transfected in HaCaT cells. This assay is based on the Tetracycline-Regulated Expression system (Tet-On system), and the expression of GLI1 is regulated by a tetracycline repressor. The addition of tetracycline produces exogenous GLI1 proteins in the assay cell, and subsequently luciferase expression is increased. Cells (HaCaT-GLI1-luc) were cultured in a 96-well white plate at 2 × 10^4 cells per well at 37 °C for 12 h. After incubation, 1 μg mL^{-1} tetracycline was added to each well to express exogenous GLI1 protein, and cells were incubated at 37 °C for 12 h. The medium was replaced with tetracycline-free medium containing different concentrations of each sample. After treatment at 37 °C for 12 h, luciferase activity was measured using a microplate luminometer (Thermo) using the Bright-Glo™ Luciferase Assay System (Promega) according to the manufacturer's protocol. The ratio of the reporter luciferase activity of sample-treated cells/non-treated cells was calculated as GLI1-mediated transcriptional activity. At the same time, the cell viability of the sample-treated cells was measured. The same cells (HaCaT-GLI1-luc) were seeded onto a 96-well black plate at 2 × 10^4 cells per well at 37 °C for 24 h. Different concentrations of samples were added at the same time as the luciferase assay, and the cells were incubated at 37 °C for 12 h. Cell viability was determined by FMCA using a fluorescence plate reader (Thermo). The ratio of sample-treated cells/non-treated cells was calculated as cell viability.

Western blotting analysis

PANC1 cells were seeded onto a 10 cm dish at 2 × 10^6 cells, and pre-incubated at 37 °C for 24 h. The medium was then changed to new medium including the compound. After 24 h treatment of compounds, cells were washed with PBS and then homogenized in lysis buffer (20 mM Tris-HCl (pH 7.4), 150 mM NaCl, 0.5% Triton X-100, 0.5% sodium deoxycholate, 10 mM EDTA, 1 mM sodium orthovanadate, and 0.1 mM NaF) containing 1% proteasome inhibitor cocktail (Nacalai Tesque, Tokyo, Japan), and incubated on ice for 30 min. The cell lysate were centrifuged for 30 min at 4 °C, and the supernatants were resolved by electrophoresis on 7.5% and 12.5% polyacrylamide gels and transferred to a polyvinylidine difluoride (PVDF) membrane (Bio-Rad). After blocking with TBST (10 mM Tris-HCl, pH 7.4, 100 mM NaCl, and 0.1% Tween 20) containing 5% skimmed milk for 1 h at room temperature, the blots were hybridized at room temperature for 1 h with primary antibodies. β-Actin was used as an internal control. After washing with TBST, the blots were incubated at room temperature for 1 h with secondary antibodies conjugated with horseradish peroxidase. After washing, the immunocomplexes were visualized using an ECL Advance Western detection system (GE Healthcare/Amersham Biosciences) or Immobilon Western (Millipore). Analysis was performed using antibodies to PTCH (1:200) (Santa Cruz Biotechnology, Santa Cruz, CA, USA), and BCL2 (1:4000) (Sigma) as primary antibodies, and anti-goat IgG (Sigma), anti-rabbit IgG and anti-mouse IgG (Amersham Biosciences) as secondary antibodies.

Cytotoxicity test

PANC1 and C3H10T1/2 were from RIKEN BRC. DU145 were from the Cell Resource Center for Biomedical Research Institute of Development, Aging and Cancer, Tohoku University. Cells (PANC1, DU145 and C3H10T1/2) were seeded onto a 96-well black plate at 1 × 10^4 cells per well, and pre-incubated at 37 °C for 24 h. The medium was replaced with fresh medium containing different concentrations of each compound, and the cells were incubated at 37 °C for 24 h. After the medium was removed, cell proliferation was determined by FMCA using a fluorescence plate

reader (Thermo). The ratio of living cells was determined as the fluorescence in the sample wells expressed as a percentage of that in the control cells, and cytotoxic activity was indicated as an IC_{50} value.

RNA isolation and real time RT-PCR analysis

Total RNA was isolated from PANC1 cells treated with compounds using the RNeasy Mini Kit (Qiagen) according to the manufacturer's protocol. cDNA was synthesized and RT-PCR reactions were performed using the RT-PCR SuperScript III Platinum Two-Step qRT-PCR Kit (Invitrogen) according to the manufacturer's instructions. The reactions were performed using an Mx3000P QPCR System (Stratagene), using the following RT-PCR program: 50 °C for 2 min (initial incubation), 95 °C for 2 min (initial denaturation), and then 40 cycles of 95 °C for 15 s (denaturation) and 60 °C for 30 s (annealing, extension). Sequences of the primers were as follows: *PTCH*; 5′-TCCTCGTGTGCGCTGTCTTCCTTC-3′ and 5′-CGTCAGAAAGGCCAAAGCAACGTGA-3′ (200 bp product), and human *GAPDH*; 5′-ATGGGGAAGGTGAAGGTCG-3′ and 5′-TAAAAGCAGCCCTGGTGACC-3′ (70 bp product) as an internal control. A fluorescence signal was collected at the end of each cycle. After the reactions were terminated, the signal at each temperature from 60 to 95 °C was also collected for dissociation curve analysis. All reactions were performed in triplicate to confirm reproducibility, and the amount of target mRNA in each sample was normalized with that of the mean *GAPDH*.

Acknowledgements

We are very grateful to Drs. Fritz Aberger and Gerhard Regl (University of Salzburg) for the kind provision of tetracycline-regulated HaCaT cells, Dr. Rune Toftgård (Karolinska Institute) for the 12GLI-RE-TKO luciferase plasmid. This study was supported by Grants-in-Aid for Scientific Research from the Japan Society for the Promotion of Science (JSPS).

References

1 M. P. di Magliano and M. Hebrok, *Nat. Rev. Cancer*, 2003, **3**, 903–911.
2 M. Kasper, G. Regl, A. M. Frischauf and F. Aberger, *Eur. J. Cancer*, 2006, **42**, 437–445.
3 M. R. Gailani and A. E. Bale, *J. Natl. Cancer Inst.*, 1997, **89**, 1103–1109.
4 B. Stecca and A. Ruiz i Altaba, *J. Neurobiol.*, 2005, **64**, 476–490.
5 P. Sanchez, A. M. Hernández, B. Stecca, A. J. Kahler, A. M. DeGueme, A. Barrett, M. Beyna, M. W. Datta, S. Datta and A. Ruiz i Altaba, *Proc. Natl. Acad. Sci. U. S. A.*, 2004, **101**, 12561–12566.
6 D. M. Berman, S. S. Karhadkar, A. Maitra, R. Montes de Oca, M. R. Gerstenblith, K. Briggs, A. R. Parker, Y. Shimada, J. R. Eshleman, D. N. Watkins and P. A. Beachy, *Nature*, 2003, **425**, 846–851.
7 S. P. Thayer, M. P. di Magliano, P. W. Heiser, C. M. Nielsen, D. J. Roberts, G. Y. Lauwers, Y. P. Qi, S. Gysin, C. Fernández-del Castillo, V. Yajnik, B. Antoniu, M. McMahon, A. L. Warshaw and M. Hebrok, *Nature*, 2003, **425**, 851–856.
8 D. N. Watkins, D. M. Berman, S. G. Burkholder, B. Wang, P. A. Beachy and S. B. Baylin, *Nature*, 2003, **422**, 313–317.
9 L. L. Rubin and F. J. de Sauvage, *Nat. Rev. Drug Discovery*, 2006, **5**, 1026–1033.
10 J. K. Chen, J. Taipale, M. K. Cooper and P. A. Beachy, *Genes Dev.*, 2002, **16**, 2743–2748.
11 J. P. Incardona, W. Gaffield, R. P. Kapur and H. Roelink, *Development*, 1998, **125**, 3553–3556.
12 J. A. Williams, O. M. Guicherit, B. I. Zaharian, Y. Xu, L. Chai, H. Wichterle, C. Kon, C. Gatchalian, J. A. Porter, L. L. Rubin and F. Y. Wang, *Proc. Natl. Acad. Sci. U. S. A.*, 2003, **100**, 4616–4621.
13 J. K. Chen, J. Taipale, K. E. Young, T. Maiti and P. A. Beachy, *Proc. Natl. Acad. Sci. U. S. A.*, 2002, **99**, 14071–14076.
14 M. Lauth, Å. Bergström, T. Shimokawa and R. Toftgård, *Proc. Natl. Acad. Sci. U. S. A.*, 2007, **104**, 8455–8460.
15 J. Lee, X. Wu, M. Pasca di Magliano, E. C. Peters, Y. Wang, J. Hong, M. Hebrok, S. Ding, C. Y. Cho and P. G. Schultz, *ChemBioChem*, 2007, **8**, 1916–1919.
16 B. Z. Stanton, L. F. Peng, N. Maloof, K. Nakai, X. Wang, J. L. Duffner, K. M. Taveras, J. M. Hyman, S. W. Lee, A. N. Koehler, J. K. James K Chen, J. L. Fox, A. Mandinova and S. L. Schreiber, *Nat. Chem. Biol.*, 2009, **5**, 154–156.
17 T. Hosoya, M. A. Arai, T. Koyano, T. Kowithayakorn and M. Ishibashi, *ChemBioChem*, 2008, **9**, 1082–1092.
18 R. M. Pádua, A. B. Oliveira, J. D. S. Filho, G. J. Vieira, J. A. Takahashi and F. C. Braga, *J. Braz. Chem. Soc.*, 2005, **16**, 614–619.
19 T. Yamauchi and F. Abe, *Chem. Pharm. Bull.*, 1990, **38**, 1140–1142.
20 A. Aebi and T. Reichstein, *Helv. Chim. Acta*, 1950, **33**, 1013–1034.
21 M. Zhao, L. Bai, L. Wang, A. Toki, T. Hasegawa, M. Kikuchi, M. Abe, J. Sakai, R. Hasegawa, Y. Bai, T. Mitsui, H. Ogura, T. Kataoka, S. Oka, H. Tsushima, M. Kiuchi, K. Hirose, A. Tomida, T. Tsuruo and M. Ando, *J. Nat. Prod.*, 2007, **70**, 1098–1103.
22 T. Yamauchi and F. Abe, *Chem. Pharm. Bull.*, 1990, **38**, 669–672.
23 Y. C. Kim, R. Higuchi, T. Komori, F. Abe and T. Yamauchi, *Liebigs Ann. Chem.*, 1990, **9**, 943–947.
24 K. Reyle and T. Reichstein, *Helv. Chim. Acta*, 1952, **35**, 195–214.
25 K. Friedhelm, *Chem. Ber.*, 1955, **88**, 1527–1534.
26 R. Larsson, J. Kristensen, C. Sandberg and P. Nygren, *Int. J. Cancer*, 1992, **50**, 177–185.
27 R. L. Bigelow, N. S. Chari, A. B. Unden, K. B. Spurgers, S. Lee, D. R. Roop, R. Toftgård and T. J. McDonnell, *J. Biol. Chem.*, 2004, **279**, 1197–1205.
28 G. Regl, M. Kasper, H. Schnidar, T. Eichberger, G. W. Neill, M. P. Philpott, H. Esterbauer, C. Hauser-Kronberger, A. M. Frischauf and F. Aberger, *Cancer Res.*, 2004, **64**, 7724–7731.